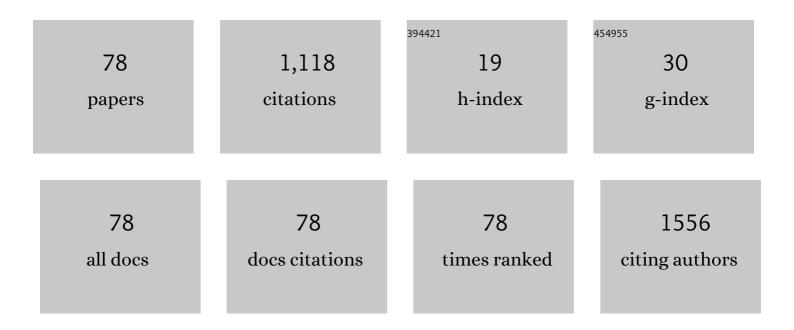
## Dao-Hua Zhang

List of Publications by Year in descending order

Source: https://exaly.com/author-pdf/5197458/publications.pdf Version: 2024-02-01



#	Article	IF	CITATIONS
1	Plasmonic semiconductor nanogroove array enhanced broad spectral band millimetre and terahertz wave detection. Light: Science and Applications, 2021, 10, 58.	16.6	32
2	Great Enhancement Effect of 20–40 nm Ag NPs on Solar-Blind UV Response of the Mixed-Phase MgZnO Detector. ACS Omega, 2021, 6, 6699-6707.	3.5	4
3	Nearly total optical transmission of linearly polarized light through transparent electrode composed of GaSb monolithic high-contrast grating integrated with gold. Nanophotonics, 2021, 10, 3823-3830.	6.0	4
4	Hybridized surface lattice modes in intercalated 3-disk plasmonic crystals for high figure-of-merit plasmonic sensing. Nanoscale, 2021, 13, 4092-4102.	5.6	9
5	Controlling Spontaneous Emission from Perovskite Nanocrystals with Metal–Emitter–Metal Nanostructures. Crystals, 2021, 11, 1.	2.2	17
6	Si metasurface half-wave plates demonstrated on a 12-inch CMOS platform. Nanophotonics, 2020, 9, 149-157.	6.0	28
7	Strong Plasmon–Exciton Interactions on Nanoantenna Array–Monolayer WS <sub>2</sub> Hybrid System. Advanced Optical Materials, 2020, 8, 1901002.	7.3	28
8	Effect of Size on the Electronic Structure and Optical Properties of Cubic CsPbBr <sub>3</sub> Quantum Dots. IEEE Journal of Quantum Electronics, 2020, 56, 1-7.	1.9	3
9	GeSn/GaAs Hetero-Structure by Magnetron Sputtering. IEEE Journal of Quantum Electronics, 2020, 56, 1-5.	1.9	1
10	Growth of Direct Bandgap Ge1â^'xSnx Alloys by Modified Magnetron Sputtering. IEEE Journal of Quantum Electronics, 2020, 56, 1-4.	1.9	0
11	Dark Current Analysis of InAsSb-Based Hetero-\$p{ext{-}}i{ext{-}}n\$ Mid-Infrared Photodiode. IEEE Journal of Quantum Electronics, 2020, 56, 1-6.	1.9	0
12	Resonance Modes of Tall Plasmonic Nanostructures and Their Applications for Biosensing. IEEE Journal of Quantum Electronics, 2020, 56, 1-7.	1.9	3
13	Band Structure of Strained \$mathrm{Ge}_{1-x}~mathrm{Sn}_{x}\$ Alloy: A Full-Zone 30-Band \${k}cdot{p}\$ Model. IEEE Journal of Quantum Electronics, 2020, 56, 1-8.	1.9	4
14	Polarization-Controlled Plasmonic Structured Illumination. Nano Letters, 2020, 20, 2602-2608.	9.1	29
15	Virtual Special Issue Dedicated to the 10th International Conference on Materials for Advanced Technologies (ICMAT), Symposium C: Semiconductor Photonics. IEEE Journal of Quantum Electronics, 2020, 56, 1-3.	1.9	0
16	High Order Magnetic and Electric Resonant Modes of Split Ring Resonator Metasurface Arrays for Strong Enhancement of Mid-Infrared Photodetection. ACS Applied Materials & Interfaces, 2020, 12, 8835-8844.	8.0	13
17	Hybrid Transverse–Longitudinal Modes for High Figureâ€ofâ€Merit Localized Plasmonic Refractometric Sensing in the Visible Spectrum. Advanced Optical Materials, 2020, 8, 1901739.	7.3	6
18	Manipulating Coherent Light–Matter Interaction: Continuous Transition between Strong Coupling and Weak Coupling in MoS <sub>2</sub> Monolayer Coupled with Plasmonic Nanocavities. Advanced Optical Materials, 2019, 7, 1900857.	7.3	48

#	Article	IF	CITATIONS
19	Ultrathin Highly Luminescent Twoâ€Monolayer Colloidal CdSe Nanoplatelets. Advanced Functional Materials, 2019, 29, 1901028.	14.9	56
20	Broadband Absorption Tailoring of SiO2/Cu/ITO Arrays Based on Hybrid Coupled Resonance Mode. Nanomaterials, 2019, 9, 852.	4.1	5
21	Ultrathin Dual-Band Metasurface Polarization Converter. IEEE Transactions on Antennas and Propagation, 2019, 67, 4636-4641.	5.1	120
22	Concurrent Inhibition and Redistribution of Spontaneous Emission from All Inorganic Perovskite Photonic Crystals. ACS Photonics, 2019, 6, 1331-1337.	6.6	39
23	Plasmon–exciton systems with high quantum yield using deterministic aluminium nanostructures with rotational symmetries. Nanoscale, 2019, 11, 20315-20323.	5.6	4
24	Asymmetric Split H-Shape Resonator Array for Enhancement of Midwave Infrared Photodetection. IEEE Journal of Quantum Electronics, 2019, 55, 1-6.	1.9	1
25	Reliable Fabrication of High Aspect Ratio Plasmonic Nanostructures Based on Seedless Pulsed Electrodeposition. Advanced Materials Technologies, 2019, 4, 1800364.	5.8	10
26	Antenna-assisted subwavelength metal–InGaAs–metal structure for sensitive and direct photodetection of millimeter and terahertz waves. Photonics Research, 2019, 7, 89.	7.0	11
27	Surface plasmon enhanced infrared photodetection. Opto-Electronic Advances, 2019, 2, 18002601-18002610.	13.3	53
28	Localized surface plasmon enhanced infrared photodetectors for uncooled imaging systems. , 2019, , .		0
29	Polarization-Resolved Plasmon-Modulated Emissions of Quantum Dots Coupled to Aluminum Dimers with Sub-20 nm Gaps. ACS Photonics, 2018, 5, 1566-1574.	6.6	17
30	Combining sonicated cold development and pulsed electrodeposition for high aspect ratio sub-10 nm gap gold dimers for sensing applications in the visible spectrum. Nanoscale, 2018, 10, 5221-5228.	5.6	13
31	Single Plasmonic Structure Enhanced Dual-band Room Temperature Infrared Photodetection. Scientific Reports, 2018, 8, 1548.	3.3	14
32	High quality InAsSb-based heterostructure n-i-p mid-wavelength infrared photodiode. Applied Surface Science, 2018, 427, 605-608.	6.1	19
33	Defect-Induced Tunable Permittivity of Epsilon-Near-Zero in Indium Tin Oxide Thin Films. Nanomaterials, 2018, 8, 922.	4.1	20
34	InAs0.9Sb0.1-based hetero-p-i-n structure grown on GaSb with high mid-infrared photodetection performance at room temperature. Journal of Materials Science, 2018, 53, 13010-13017.	3.7	7
35	Electrically controlled enhancement in plasmonic mid-infrared photodiode. Optics Express, 2018, 26, 5452.	3.4	11
36	Room temperature plasmon-enhanced InAs0.91Sb0.09-based heterojunction <i>n-i-p</i> mid-wave infrared photodetector. Applied Physics Letters, 2018, 113, .	3.3	21

#	Article	IF	CITATIONS
37	Study of dark current in mid-infrared InAsSb-based hetero <i>n</i> - <i>i</i> - <i>p</i> photodiode. Journal Physics D: Applied Physics, 2018, 51, 275102.	2.8	10
38	A Simple Method for the Growth of Very Smooth and Ultra-Thin GaSb Films on GaAs (111) Substrate by MOCVD. Journal of Electronic Materials, 2017, 46, 3867-3872.	2.2	3
39	Multifunctional Hyperbolic Nanogroove Metasurface for Submolecular Detection. Small, 2017, 13, 1700600.	10.0	46
40	Polarization invariant plasmonic nanostructures for sensing applications. Scientific Reports, 2017, 7, 7539.	3.3	21
41	Ultra-small v-shaped gold split ring resonators for biosensing using fundamental magnetic resonance in the visible spectrum. Nanotechnology, 2017, 28, 405305.	2.6	11
42	Surface plasmon induced direct detection of long wavelength photons. Nature Communications, 2017, 8, 1660.	12.8	51
43	Room temperature strong coupling of monolayer WS <inf>2</inf> with gold nanoantennae. , 2017, , .		0
44	Preferential Excitation of the Hybrid Magnetic–Electric Mode as a Limiting Mechanism for Achievable Fundamental Magnetic Resonance in Planar Aluminum Nanostructures. Advanced Materials, 2016, 28, 889-896.	21.0	15
45	Observation of the Kinetic Inductance Limitation for the Fundamental Magnetic Resonance in Ultrasmall Gold <i>v</i> â€Shape Split Ring Resonators. Advanced Optical Materials, 2016, 4, 1047-1052.	7.3	24
46	Study of dual color infrared photodetection from n-GaSb/n-InAsSb heterostructures. AIP Advances, 2016, 6, 025120.	1.3	10
47	On-chip photonic Fourier transform with surface plasmon polaritons. Light: Science and Applications, 2016, 5, e16034-e16034.	16.6	58
48	Surface Plasmon Enhancement on Infrared Photodetection. Procedia Engineering, 2016, 140, 152-158.	1.2	7
49	InAs <sub>0.91</sub> Sb <sub>0.09</sub> photoconductor for near and middle infrared photodetection. Physica Scripta, 2016, 91, 115801.	2.5	4
50	Surface-enhanced Raman scattering of silver thin films on as-roughened substrate by reactive ion etching. Applied Physics A: Materials Science and Processing, 2016, 122, 1.	2.3	7
51	Two-dimensional metallic square-hole array for enhancement of mid-wavelength infrared photodetection. Optical and Quantum Electronics, 2016, 48, 1.	3.3	6
52	On-chip discrimination of orbital angular momentum of light with plasmonic nanoslits. Nanoscale, 2016, 8, 2227-2233.	5.6	76
53	A sensitive sensor with a double U-shaped ring-based metamaterial. Applied Physics A: Materials Science and Processing, 2014, 117, 537-540.	2.3	2
54	Subâ€100â€nm Sized Silver Split Ring Resonator Metamaterials with Fundamental Magnetic Resonance in the Middle Visible Spectrum. Advanced Optical Materials, 2014, 2, 280-285.	7.3	25

#	Article	IF	CITATIONS
55	Figure of Merit for Optimization of Metal–Dielectric Multilayer Lenses. IEEE Nanotechnology Magazine, 2014, 13, 452-457.	2.0	2
56	Sub-10-nm Size and Sub-40-nm Pitch Metal Dot Patterning for Low-Cost Bit Patterned Media Application. IEEE Nanotechnology Magazine, 2014, 13, 496-501.	2.0	7
57	Real-Time Angular Sensitivity Compensation of Guided-Mode Resonance Filter. IEEE Photonics Technology Letters, 2014, 26, 231-234.	2.5	12
58	Sub-wavelength structures and their optical properties. , 2014, , .		0
59	Design of sharp bends with transformation plasmonics. Applied Physics A: Materials Science and Processing, 2013, 112, 549-553.	2.3	4
60	The new way of controlling aluminum-doped zinc oxide films properties: ion beam post-treatment with cooling system. Applied Physics A: Materials Science and Processing, 2013, 112, 569-573.	2.3	0
61	Manipulating Surface Plasmon Polaritons on the meta-surface. , 2013, , .		0
62	Beam focusing by an anisotropic metal-dielectric multilayer structure. , 2013, , .		0
63	Large contrast enhancement by sonication assisted cold development process for low dose and ultrahigh resolution patterning on ZEP520A positive tone resist. Journal of Vacuum Science and Technology B:Nanotechnology and Microelectronics, 2012, 30, 051601.	1.2	17
64	The substrate cooling effect of ion beam post treatment on ZAO films properties. , 2012, , .		0
65	Designing arbitrary nanoscale patterns by a nanocavity waveguide with omnidirectional illumination. Applied Physics B: Lasers and Optics, 2012, 109, 215-219.	2.2	7
66	Elimination of spurious solutions from k·p theory with Fourier transform technique and Burt-Foreman operator ordering. Journal of Applied Physics, 2012, 111, 053702.	2.5	6
67	Efficient and wide spectrum half-cylindrical hyperlens with symmetrical metallodielectric structure. Applied Physics A: Materials Science and Processing, 2012, 107, 31-34.	2.3	4
68	Subwavelength lithography using metallic grating waveguide heterostructure. Applied Physics A: Materials Science and Processing, 2012, 107, 123-126.	2.3	5
69	Analysis of wetting layer effect on electronic structures of truncated-pyramid quantum dots. Optical and Quantum Electronics, 2011, 42, 705-711.	3.3	3
70	Subwavelength Focusing Using Plasmonic Wavelength-Launched Zone Plate Lenses. Plasmonics, 2011, 6, 269-272.	3.4	7
71	Beam splitting and a hollow light cone from a metamaterial based on a metallic nanorod array. , 2010, ,		0

1

#	Article	IF	CITATIONS
73	Study of InAs/GaAs quantum dots grown by MOVPE under the safer growth conditions. Journal of Nanoparticle Research, 2007, 9, 877-884.	1.9	2
74	Mid-Infrared Emission From InAs Quantum Dots Grown by Metal–Organic Vapor Phase Epitaxy. IEEE Nanotechnology Magazine, 2006, 5, 683-686.	2.0	3
75	Temperature dependence of BaTiO3 infrared dielectric properties. Applied Physics Letters, 2006, 88, 212902.	3.3	7
76	A Novel Technique to Re-construct 3D Void in Passivated Metal Interconnects. Materials Research Society Symposia Proceedings, 2003, 766, 481.	0.1	1
77	Six-band k/spl middot/p approach to the effects of doping on energy dispersion in p-type strained In/sub 0.15/Ga/sub 0.85/As-Al/sub 0.33/Ga/sub 0.67/As quantum-well structures. IEEE Journal of Quantum Electronics, 2000, 36, 835-841.	1.9	1
78	Interplays of Dipole and Chargeâ€Transferâ€Plasmon Modes in Capacitively and Conductively Coupled Dimer with High Aspect Ratio Nanogaps. Advanced Optical Materials, 0, , 2100748.	7.3	3